PERGAMON

International Journal of Solids and Structures 38 (2001) 741–757

INTERNATIONAL JOURNAL OF SOLIDS and STRUCTURES

www.elsevier.com/locate/ijsolstr

Plastic buckling of circular cylindrical shells under combined in-plane loads

Renjie Mao [a,*,1], G. Lu [b]

[a] Department of Engineering Mechanics, Shanghai Jiao Tong University, Shanghai 200030, People's Republic of China
[b] School of Engineering and Science, Swinburne University of Technology, Hawthorn, Vic. 3122, Australia

Received 6 February 1999; in revised form 18 September 1999

Abstract

A study of plastic buckling of a circular cylindrical shell subject to axial, torsional and circumferential loading stresses is presented. In the deformation model, the transverse shear is taken into account by a first-order theory with a correction factor. For the buckled equilibrium, the contributions of both v (circumferential displacement) and w (normal displacement) to the buckling are included so that a better accuracy can be achieved. J_2 deformation theory and J_2 flow theory of plasticity are used for the establishment of the constitutive relations for buckling analysis. With the existence of torsional load, the equation of radial equilibrium includes the term of mixed second-order derivative $\partial^2 w/\partial x \partial y$ and the plastic in-plane stress–strain relations are anisotropic, and therefore a handy form of solution in terms of trigonometric functions is no longer possible. Consequently, the finite difference method is used. To improve the accuracy, a five-point finite difference scheme is employed instead of the conventional central difference. Numerical results of examples show the interactive roles of the in-plane loads in the plastic buckling. © 2001 Elsevier Science Ltd. All rights reserved.

Keywords: Plastic buckling; Shell structure

1. Introduction

The plastic buckling problem of a circular cylindrical shell has long been widely investigated due to its great importance in the design of aerospace and marine structures. The investigations have in turn greatly promoted the development of the theory and method in dealing with the buckling phenomenon in the past half a century. Numerous works about this problem can be found in the literature, covering theoretical and experimental studies of elastic and plastic buckling under the loads of axial compression, external pressure or end torsion. For the plastic buckling, among other recent works, studies by Andrews et al. (1983), Ore and Durban (1992) and Lin and Yeh (1994) are worth mentioning. They are all concerned with the buckling

* Corresponding author. Fax: +86-6282-0892.
E-mail addresses: rjmao@srcap.stc.sh.cn (R. Mao), glu@swin.edu.au (G. Lu).
[1] Currently visiting research professor, School of Engineering and Science, Swinburne University of Technology.

PII: S0020-7683(00)00041-X

under axial compression and are typical of experimental, analytical and numerical methods, respectively. For plastic buckling under combined loads especially in the case when torsion is involved, not as many previous works can be found as in the case without torsion. This is partly because of two difficulties arising from the existence of torsion. First, the equation of buckled equilibrium in the normal direction will thus include the mixed second-order derivative $\partial^2 w/\partial x \partial y$. Second, the prebuckling stress state will thus include shear stress and the stress–strain relations will become anisotropic when the shell is loaded into plastic range. With these difficulties, the equations of buckled equilibrium cannot be solved in terms of simple trigonometric or exponential functions, but must be treated with numerical methods. Teng and Rotter (1989) gave a detailed account of the use of finite element method for the bifurcation analysis of elastic–plastic axisymmetric shells under combined loads including torsion. Tuğcu (1985, 1991) used a helical form for the displacements of buckling, disregarding the end conditions, to predict the bifurcation of elastic–plastic cylindrical shells under combined loading, including axial, radial and torsional loads. The results are good as long as the effect of end conditions can be ignored. Lee and Ades (1957) presented a series of experimental results of plastic buckling of cylindrical shells under pure torsion, accompanied by a theoretical analysis with the energy method under some simplification for stress–strain relations. For the plastic buckling of shells with bi-axial prebuckling stress state, in addition to Tuğcu (1985, 1991) mentioned above, Giezen et al. (1991) and Blachut et al. (1996) studied cylindrical shells subjected to external pressure and axial tension with a special attention to the nonproportional loading effect and the well known plastic buckling paradox regarding the deformation theory and the flow theory.

In the present paper, the plastic buckling of a circular cylindrical shell under combined axial, torsional and circumferential loading stresses is studied. The axial and circumferential loads may be compressive or tensile. The deformation model used for analysis is the so-called first-order shear deformation theory, which allows for the transverse shear of the shell, so that there are five independent variables involved in the problem, namely, three displacements and two rotations. As a result, there are five equations for the buckled equilibrium. In these equations, the contribution of a term involving $\partial^2 v/\partial x^2$ to the buckling is included. The inclusion of this term may improve the accuracy in predicting the critical load especially in the case of column-type buckling (Mao and Williams, 1998a). In addition, due to the existence of torsion, these equations include the mixed derivative $\partial^2 w/\partial x \partial y$ and plastic stress–strain relations become anisotropic. Therefore, these equations cannot be fully solved in the form of trigonometric functions. The main task of the present study is to solve the complete set of five equations together with the anisotropic stress–strain relations. To do this, a semi-analytical method is used. By assuming a trigonometric form in the circumferential direction, the equations of buckled equilibrium are reduced to ordinary differential equations in the axial direction, which are solved with a five-point finite difference scheme.

The computer code based on the foregoing theory and method is checked against some available experimental data for cases of individual load. Numerical results of examples are given with special focus on the interactive roles of the loads as stabilizing or destabilizing factors.

2. Basic equations

A right-handed axis system is used for a circular cylindrical shell of radius R and length L. Let x, θ and z be the coordinates for any point P in the shell wall, where x is the axial distance of the point to one end of the shell, θ is the circumferential angular coordinate and z is the distance of the point to the middle surface (positive when the point is on the outer side of the middle surface). Another circumferential coordinate $y = R\theta$ is also used.

The displacement field of the first-order shear-deformation theory assumes that

$$
\begin{aligned}
u^*(x,y,z) &= u(x,y) + z\psi(x,y), \\
v^*(x,y,z) &= v(x,y) + z\varphi(x,y), \\
w^*(x,y,z) &= w(x,y),
\end{aligned}
\tag{1}
$$

where $\{u^*, v^*, w^*\}$ is the displacement vector in the (x,y,z) coordinate system at an arbitrary point $P(x,y,z)$. The associated strains at $P(x,y,z)$ in the case of small strains and finite rotations are given by Mao and Williams (1998b) for thick shells. For thin shells, it reduces to

$$
\begin{aligned}
\varepsilon_x^*(x,y,z) &= \varepsilon_x(x,y) + z\frac{\partial\psi(x,y)}{\partial x}, \\
\varepsilon_y^*(x,y,z) &= \varepsilon_y(x,y) + z\frac{\partial\varphi(x,y)}{\partial y}, \\
\gamma_{xy}^*(x,y,z) &= \gamma_{xy}(x,y) + z\left(\frac{\partial\psi(x,y)}{\partial y} + \frac{\partial\varphi(x,y)}{\partial x}\right), \\
\gamma_{xz}^*(x,y,z) &= \gamma_{xz}(x,y) = \frac{\partial w}{\partial x} + \psi, \\
\gamma_{yz}^*(x,y,z) &= \gamma_{yz}(x,y) = \frac{\partial w}{\partial y} - \frac{v}{R} + \varphi,
\end{aligned}
\tag{2}
$$

where

$$
\begin{aligned}
\varepsilon_x &= \frac{\partial u}{\partial x} + \frac{1}{2}\left[\left(\frac{\partial v}{\partial x}\right)^2 + \left(\frac{\partial w}{\partial x}\right)^2\right], \\
\varepsilon_y &= \frac{\partial v}{\partial y} + \frac{w}{R} + \frac{1}{2}\left(\frac{\partial w}{\partial y} - \frac{v}{R}\right)^2, \\
\gamma_{xy} &= \frac{\partial u}{\partial y} + \frac{\partial v}{\partial x} + \frac{\partial w}{\partial x}\left(\frac{\partial w}{\partial y} - \frac{v}{R}\right)
\end{aligned}
\tag{3a}
$$

represent the strains at the middle surface. In the linearized case, these strains can be further simplified to become

$$
\varepsilon_x = \frac{\partial u}{\partial x}, \quad \varepsilon_y = \frac{\partial v}{\partial y} + \frac{w}{R}, \quad \gamma_{xy} = \frac{\partial u}{\partial y} + \frac{\partial v}{\partial x}. \tag{3b}
$$

Based on the nonlinear kinematic equation (2) application of the principle of virtual work yields the equations of buckled equilibrium (Mao and Williams, 1998a,b).

$$
\frac{\partial T_x}{\partial x} + \frac{\partial T_{xy}}{\partial y} = 0, \tag{4a}
$$

$$
\frac{\partial T_{xy}}{\partial x} + \frac{\partial T_y}{\partial y} + \frac{Q_y}{R} + \frac{\partial}{\partial x}\left(T_x\frac{\partial v}{\partial x}\right) + \frac{T_y}{R}\left(\frac{\partial w}{\partial y} - \frac{v}{R}\right) + \frac{T_{xy}}{R}\frac{\partial w}{\partial x} = 0, \tag{4b}
$$

$$
\frac{\partial Q_x}{\partial x} + \frac{\partial Q_y}{\partial y} - \frac{T_y}{R} + \frac{\partial}{\partial x}\left(T_x\frac{\partial w}{\partial x}\right) + \frac{\partial}{\partial y}\left[T_y\left(\frac{\partial w}{\partial y} - \frac{v}{R}\right)\right] + \frac{\partial}{\partial x}\left[T_{xy}\left(\frac{\partial w}{\partial y} - \frac{v}{R}\right)\right] + \frac{\partial}{\partial y}\left(T_{xy}\frac{\partial w}{\partial x}\right) = 0, \tag{4c}
$$

$$\frac{\partial M_x}{\partial x} + \frac{\partial M_{xy}}{\partial y} - Q_x = 0, \tag{4d}$$

$$\frac{\partial M_{xy}}{\partial x} + \frac{\partial M_y}{\partial y} - Q_y = 0, \tag{4e}$$

where the stress resultants are defined as usual

$$T_x = \int_{-h/2}^{h/2} \sigma_x^* \mathrm{d}z, \quad M_x = \int_{-h/2}^{h/2} \sigma_x^* z \, \mathrm{d}z, \quad Q_x = \int \tau_{xz}^* \mathrm{d}z, \ldots \text{etc.} \tag{5}$$

and h is the thickness of the shell. The stresses with a superscript star in Eq. (5) are those at an arbitrary point $P(x, y, z)$.

Eqs. (4a)–(4e) are similar to their corresponding equations in Stein (1986) with the only difference being that Eq. (4b) includes an additional nonlinear term, $\partial/\partial x(T_x \partial v/\partial x)$, which may improve the accuracy in predicting the critical load, especially in the case of column-type buckling (Mao and Williams, 1998a).

From Eqs. (4a)–(4e) a set of Donnell-type nonlinear equations of equilibrium can be obtained by dropping these nonlinear terms which do not include the second-order derivatives of displacements,

$$\frac{\partial T_x}{\partial x} + \frac{\partial T_{xy}}{\partial y} = 0, \tag{6a}$$

$$\frac{\partial T_{xy}}{\partial x} + \frac{\partial T_y}{\partial y} + \frac{Q_y}{R} + \frac{\partial}{\partial x}\left(T_x \frac{\partial v}{\partial x}\right) = 0, \tag{6b}$$

$$\frac{\partial Q_x}{\partial x} + \frac{\partial Q_y}{\partial y} - \frac{T_y}{R} + \frac{\partial}{\partial x}\left(T_x \frac{\partial w}{\partial x}\right) + \frac{\partial}{\partial x}\left(T_{xy} \frac{\partial w}{\partial y}\right) + \frac{\partial}{\partial y}\left(T_{xy} \frac{\partial w}{\partial x}\right) + \frac{\partial}{\partial y}\left(T_y \frac{\partial w}{\partial y}\right) = 0, \tag{6c}$$

$$\frac{\partial M_x}{\partial x} + \frac{\partial M_{xy}}{\partial y} - Q_x = 0, \tag{6d}$$

$$\frac{\partial M_{xy}}{\partial x} + \frac{\partial M_y}{\partial y} - Q_y = 0. \tag{6e}$$

Eqs. (6a)–(6e) agree with the equations used by Tabiei and Simitses (1994) for thin shells, except for the additional term mentioned above.

As usual, the linearized equations of equilibrium for initial buckling can be obtained from the nonlinear Equations (6a)–(6e) by replacing the stress resultants T_x, T_y and T_{xy} in the nonlinear terms of Eqs. (6b) and (6c) with the constant prebuckling membrane forces T_x^0, T_y^0 and T_{xy}^0, respectively, and take the form.

$$\frac{\partial T_x}{\partial x} + \frac{\partial T_{xy}}{\partial y} = 0, \tag{7a}$$

$$\frac{\partial T_{xy}}{\partial x} + \frac{\partial T_y}{\partial y} + \frac{Q_y}{R} + T_x^0 \frac{\partial^2 v}{\partial x^2} = 0, \tag{7b}$$

$$\frac{\partial Q_x}{\partial x} + \frac{\partial Q_y}{\partial y} - \frac{T_y}{R} + T_x^0 \frac{\partial^2 w}{\partial x^2} + 2T_{xy}^0 \frac{\partial^2 w}{\partial x \partial y} + T_y^0 \frac{\partial^2 w}{\partial y^2} = 0, \tag{7c}$$

$$\frac{\partial M_x}{\partial x} + \frac{\partial M_{xy}}{\partial y} - Q_x = 0, \tag{7d}$$

$$\frac{\partial M_{xy}}{\partial x} + \frac{\partial M_y}{\partial y} - Q_y = 0. \tag{7e}$$

As in the usual formulation of a buckling problem, the stress resultants $T_x, T_{xy}, \ldots, Q_y$ and the displacements v and w in Eqs. (7a)–(7e) are the increments of these quantities due to buckling (from the prebuckling state to a neighboring buckled state). Therefore, for the study of initial buckling, these increments can be infinitesimal.

As mentioned in the previous section, the in-plane plastic stress–strain relations are anisotropic due to the torsion. Therefore, the stress–strain relations for the shell buckling can be expressed by

$$\begin{Bmatrix} \sigma_x^* \\ \sigma_y^* \\ \tau_{xy}^* \end{Bmatrix} = \begin{bmatrix} Q_{11} & Q_{12} & Q_{16} \\ Q_{12} & Q_{22} & Q_{26} \\ Q_{16} & Q_{26} & Q_{66} \end{bmatrix} \begin{Bmatrix} \varepsilon_x^* \\ \varepsilon_y^* \\ \gamma_{xy}^* \end{Bmatrix} \tag{8a}$$

plus a separate set for transverse shear stresses and strains

$$\begin{Bmatrix} \tau_{yz}^* \\ \tau_{xz}^* \end{Bmatrix} = \begin{bmatrix} Q_{44} & 0 \\ 0 & Q_{55} \end{bmatrix} \begin{Bmatrix} \gamma_{yz}^* \\ \gamma_{xz}^* \end{Bmatrix}. \tag{8b}$$

Substituting Eqs. (8a) and (8b) into Eq. (5) gives

$$\begin{Bmatrix} T_x \\ T_y \\ T_{xy} \end{Bmatrix} = \begin{bmatrix} A_{11} & A_{12} & A_{16} \\ A_{12} & A_{22} & A_{26} \\ A_{16} & A_{26} & A_{66} \end{bmatrix} \begin{Bmatrix} \varepsilon_x \\ \varepsilon_y \\ \gamma_{xy} \end{Bmatrix}, \tag{9a}$$

$$\begin{Bmatrix} M_x \\ M_y \\ M_{xy} \end{Bmatrix} = \begin{bmatrix} D_{11} & D_{12} & D_{16} \\ D_{12} & D_{22} & D_{26} \\ D_{16} & D_{26} & D_{66} \end{bmatrix} \begin{Bmatrix} \chi_x \\ \chi_y \\ \chi_{xy} \end{Bmatrix}, \tag{9b}$$

$$\begin{Bmatrix} Q_y \\ Q_x \end{Bmatrix} = \begin{bmatrix} A_{44} & 0 \\ 0 & A_{55} \end{bmatrix} \begin{Bmatrix} \gamma_{yz} \\ \gamma_{xz} \end{Bmatrix}, \tag{10}$$

where

$$\chi_x = \frac{\partial \psi}{\partial x}, \quad \chi_y = \frac{\partial \varphi}{\partial y}, \quad \chi_{xy} = \frac{\partial \varphi}{\partial x} + \frac{\partial \psi}{\partial y}, \tag{11}$$

$$A_{ij} = \int_{-h/2}^{h/2} Q_{ij}\, dz, \quad D_{ij} = \int_{-h/2}^{h/2} Q_{ij} z^2\, dz.$$

Eq. (7a) can be satisfied by introducing a stress function F such that

$$T_x = \frac{\partial^2 F}{\partial y^2}, \quad T_{xy} = -\frac{\partial^2 F}{\partial x \partial y}. \tag{12}$$

Let F, v, w, ψ and φ be five basic unknowns of the buckling problem considered. F is used instead of u as a basic unknown for the boundary condition $T_x = 0$ (instead of $u = 0$) in this paper. This boundary condition can be satisfied more easily by F than by u. With Eq. (9a), T_y can be expressed as

$$T_y = \frac{1}{\bar{A}_{22}} (\varepsilon_y - \bar{A}_{12} T_x - \bar{A}_{26} T_{xy}), \tag{13}$$

where $[\bar{A}_{ij}]$ is the inverse of $[A_{ij}]$ in Eq. (9a). Hence, the equation of compatibility and the Eqs. (7b)–(7e) (equations of equilibrium) can also be expressed in terms of the above five basic unknowns. For initial buckling, the linearized strains of Eq. (3b) are used, from which the equation of compatibility can be obtained as

$$\frac{\partial \varepsilon_x}{\partial y} = \frac{\partial}{\partial x}\left(\gamma_{xy} - \frac{\partial v}{\partial x}\right). \tag{14}$$

Eq. (14) can be expressed in terms of the basic unknowns by

$$\begin{aligned}&\left(\bar{A}_{11}\bar{A}_{22} - \bar{A}_{12}^2\right)\frac{\partial^3 F}{\partial y^3} - 2(\bar{A}_{16}\bar{A}_{22} - \bar{A}_{12}\bar{A}_{26})\frac{\partial^3 F}{\partial x\,\partial y^2} + \left(\bar{A}_{66}\bar{A}_{22} - \bar{A}_{26}^2\right)\frac{\partial^3 F}{\partial x^2\,\partial y}\\ &\quad = \bar{A}_{26}\frac{\partial}{\partial x}\left(\frac{\partial v}{\partial y} + \frac{w}{R}\right) - \bar{A}_{12}\frac{\partial}{\partial y}\left(\frac{\partial v}{\partial y} + \frac{w}{R}\right) - \bar{A}_{22}\frac{\partial^2 v}{\partial x^2}.\end{aligned} \tag{15}$$

Similarly, Eqs. (7b)–(7e) are transformed into

$$\frac{1}{\bar{A}_{22}}\left(\frac{\partial^2 v}{\partial y^2} + \frac{1}{R}\frac{\partial w}{\partial y} - \bar{A}_{12}\frac{\partial^3 F}{\partial y^3} + \bar{A}_{26}\frac{\partial^3 F}{\partial x\,\partial y^2}\right) - \frac{\partial^3 F}{\partial x^2\,\partial y} + \frac{A_{44}}{R}\left(\frac{\partial w}{\partial y} + \varphi - \frac{v}{R}\right) + T_x^0\frac{\partial^2 v}{\partial x^2} = 0, \tag{16}$$

$$\begin{aligned}&A_{55}\left(\frac{\partial^2 w}{\partial x^2} + \frac{\partial \psi}{\partial x}\right) + A_{44}\left(\frac{\partial^2 w}{\partial y^2} + \frac{\partial \varphi}{\partial y} - \frac{1}{R}\frac{\partial v}{\partial y}\right) - \frac{1}{R\bar{A}_{22}}\left(\frac{\partial v}{\partial y} + \frac{w}{R} - \bar{A}_{12}\frac{\partial^2 F}{\partial y^2} + \bar{A}_{26}\frac{\partial^2 F}{\partial x\,\partial y}\right)\\ &\quad + T_x^0\frac{\partial^2 w}{\partial x^2} + 2T_{xy}^0\frac{\partial^2 w}{\partial x\,\partial y} + T_y^0\frac{\partial^2 w}{\partial y^2} = 0,\end{aligned} \tag{17}$$

$$D_{11}\frac{\partial^2 \psi}{\partial x^2} + (D_{12} + D_{66})\frac{\partial^2 \varphi}{\partial x\,\partial y} + D_{16}\left(2\frac{\partial^2 \psi}{\partial x\,\partial y} + \frac{\partial^2 \varphi}{\partial x^2}\right) + D_{26}\frac{\partial^2 \varphi}{\partial y^2} + D_{66}\frac{\partial^2 \psi}{\partial y^2} - A_{55}\left(\frac{\partial w}{\partial x} + \psi\right) = 0, \tag{18}$$

$$D_{22}\frac{\partial^2 \varphi}{\partial y^2} + (D_{12} + D_{66})\frac{\partial^2 \psi}{\partial x\,\partial y} + D_{26}\left(2\frac{\partial^2 \varphi}{\partial x\,\partial y} + \frac{\partial^2 \psi}{\partial y^2}\right) + D_{16}\frac{\partial^2 \psi}{\partial x^2} + D_{66}\frac{\partial^2 \varphi}{\partial x^2} - A_{44}\left(\frac{\partial w}{\partial y} + \varphi - \frac{v}{R}\right) = 0. \tag{19}$$

Eqs. (15)–(19) are the governing equations in terms of the five basic unknowns for the buckling problem considered.

3. Constitutive relations of plasticity

The most commonly used constitutive relations of plasticity for buckling problems are J_2 flow theory and J_2 deformation theory (Hill, 1983), although there is a well known paradox about their theoretical correctness and practical effectiveness.

The J_2 flow theory gives the increments of plastic strains caused by increments of stresses.

$$\mathrm{d}\varepsilon_{ij}^{\mathrm{p}} = \frac{3}{4J_2}\left(\frac{1}{E_t} - \frac{1}{E}\right)S_{ij}S_{ld}\,\mathrm{d}\sigma_{ld}. \tag{20}$$

In Eq. (20) and in Eqs. (21) and (22), the subscripts range from 1 to 3 to represent x, y and z, respectively, and the repeated subscript means summation over it from 1 to 3. The tensor S_{ij} is the stress deviator and $J_2 = S_{mn}S_{mn}/2$. E_t is the tangent modulus. For the complete constitutive relations of the J_2 flow theory, the elastic part of the incremental strains should be added to Eq. (20). As usual, when applying Eq. (20) to initial buckling problems, S_{ij} should be the deviator of the prebuckling stresses, and $\mathrm{d}\sigma_{ij}$ and $\mathrm{d}\varepsilon_{ij}^p$ should be, respectively, the increments of stresses and their associated plastic strains due to buckling. The prebuckling stress state is supposed to be a plane stress state, where $\sigma_{23} = \sigma_{31} = \sigma_{33} = 0$, and therefore Eq. (20) are greatly reduced. In particular, Eq. (20) will then give $\mathrm{d}\varepsilon_{23}^{\mathrm{p}} = \mathrm{d}\varepsilon_{31}^{p} = 0$, so that the constitutive relations (8b) and (10) are elastic.

The J_2 deformation theory usually takes the form

$$\varepsilon_{ij} = \frac{3}{2E_{\mathrm{s}}}\sigma_{ij} - \left(\frac{1}{2E_{\mathrm{s}}} - \frac{1-2v}{3E}\right)\sigma_{kk}\delta_{ij}, \tag{21}$$

where E_{s} is the secant modulus. Since buckling problems need stress–strain relations in an incremental form, Eq. (21) should be differentiated to give

$$\mathrm{d}\varepsilon_{ij} = \frac{3}{4J_2}\left(\frac{1}{E_{\mathrm{t}}} - \frac{1}{E_{\mathrm{s}}}\right)S_{ij}S_{ld}\mathrm{d}\sigma_{ld} + \frac{3}{2E_{\mathrm{s}}}\left(\mathrm{d}\sigma_{ij} - \frac{1}{3}\mathrm{d}\sigma_{kk}\delta_{ij}\right) + \frac{1-2v}{3E}\mathrm{d}\sigma_{kk}\delta_{ij}. \tag{22}$$

In the case of plane stress, Eqs. (22) are greatly reduced. It should be mentioned that the J_2 deformation theory is valid only for proportional loading, which is not always the case in buckling problems with combined loads. But as pointed out by Giezen et al. (1991), the error caused by nonproportional loading is tolerable as long as load paths do not diverge too much from a proportional path.

As usual, for initial buckling problems, it is assumed that no unloading occurs during the buckling.

4. Solution of the basic equations

The solution is assumed to be of the following form:

$$\begin{aligned}
F(x,y) &= e_c(x)\cos n\theta + e_s(x)\sin n\theta,\\
w(x,y) &= w_c(x)\cos n\theta + w_s(x)\sin n\theta,\\
v(x,y) &= v_c(x)\cos n\theta + v_s(x)\sin n\theta,\\
\psi(x,y) &= p_c(x)\cos n\theta + p_s(x)\sin n\theta,\\
\varphi(x,y) &= f_c(x)\cos n\theta + f_s(x)\sin n\theta,
\end{aligned} \tag{23}$$

where $\theta = y/R$ and n is an integer and may assume $1, 2, \ldots$ Substituting Eqs. (23) into Eqs. (15)–(19) and then letting the coefficients of $\cos n\theta$ and $\sin n\theta$ be zero for each equation yields 10 ordinary differential equations. These lengthy equations can be written in a compact matrix form as follows:

Compatibility:

$$[U^e]\{e\} = [U^v]\{v\} + [U^w]\{w\}, \tag{24a}$$

Equilibrium of forces in v-direction:

$$[V^e]\{e\} + [V^p]\{p\} + [V^f]\{f\} + [V^v]\{v\} + [V^w]\{w\} - \lambda[Y^v]\{v\} = 0, \tag{24b}$$

Equilibrium of forces in w-direction:

$$[W^e]\{e\} + [W^p]\{p\} + [W^f]\{f\} + [W^v]\{v\} + [W^w]\{w\} - \lambda[Z^w]\{w\} = 0, \tag{24c}$$

Equilibrium of moments in ψ-direction:

$$[P^p]\{p\} + [P^f]\{f\} = [P^v]\{v\} + [P^w]\{w\}, \tag{24d}$$

Equilibrium of moments in φ-direction:

$$[F^p]\{p\} + [F^f]\{f\} = [F^v]\{v\} + [F^w]\{w\}, \tag{24e}$$

where the vectors are defined as follows:

$$\{e\} = (e_c, e_s, e'_c, e'_s, e''_c, e''_s)^{\mathrm{T}} \text{ etc.}$$

and the prime is the derivative with respect to x. All the coefficient matrices $U^e, V^e, \ldots$, and F^w are 2×6 constant matrices. Their expressions are not presented in this paper for the sake of conciseness. $\lambda \geqslant 0$ is a load parameter related to the prebuckling membrane forces in the following way:

$$T_x^0 = -P\lambda, \quad T_y^0 = -Q\lambda, \quad T_{xy}^0 = S\lambda. \tag{25}$$

The deformation theory requires that P, Q and S be fixed so that $T_x^0{:}T_y^0{:}T_{xy}^0$ remain the same during the whole loading process. This is also a requirement for an eigenvalue problem to be obtained.

A five-point finite difference scheme is used to solve Eqs. (24a)–(24e). Suppose the interval concerned is divided evenly into sub-intervals by m points (called stations), $x_1, x_2, \ldots, x_m$. The derivatives of a quantity, w_c for instance, at station i can be calculated from the values of w_c at stations $i-2$, $i-1$, i, $i+1$ and $i+2$ with a five-point Lagrangian interpolation:

$$w'_c(x_i) = \frac{1}{12\Delta}(1, -8, 0, 8, -1)\{w_c^*\}, \tag{26a}$$

$$w''_c(x_i) = \frac{1}{12\Delta^2}(-1, 16, -30, 16, -1)\{w_c^*\}, \tag{26b}$$

where $\{w_c^*\} = (w_c^{i-2}, w_c^{i-1}, w_c^i, w_c^{i+1}, w_c^{i+2})^{\mathrm{T}}$ with the superscript denoting the station number, and Δ is the length of a sub-interval. Eqs. (26a) and (26b) are referred to as the "five-point central difference".

Similarly, the derivatives of w_c at x_{i-1} and x_{i-2} can be calculated with the "five-point forward difference":

$$w'_c(x_{i-1}) = \frac{1}{12\Delta}(-3, -10, 18, -6, 1)\{w_c^*\}, \tag{27a}$$

$$w''_c(x_{i-1}) = \frac{1}{12\Delta^2}(11, -20, 6, 4, -1)\{w_c^*\}, \tag{27b}$$

$$w'_c(x_{i-2}) = \frac{1}{12\Delta}(-25, 48, -36, 16, -3)\{w_c^*\}, \tag{28a}$$

$$w''_c(x_{i-2}) = \frac{1}{12\Delta^2}(35, -104, 114, -56, 11)\{w_c^*\}. \tag{28b}$$

The equations of the "five-point backward difference" for the calculation of the derivatives at x_{i+1} and x_{i+2} can be obtained from Eqs. (27a), (27b), (28a) and (28b) by reversing the direction of the x-axis.

Thus, all the vectors in Eqs. (24a)–(24e) can be expressed with the five-point finite difference scheme at any station. Finally, the differential Eqs. (24a)–(24e) are reduced to a set of algebraic equations:

$$[\bar{U}^e]\{\bar{e}\} = [\bar{U}^v]\{\bar{v}\} + [\bar{U}^w]\{\bar{w}\}, \tag{29a}$$

$$[\bar{V}^e]\{\bar{e}\} + [\bar{V}^p]\{\bar{p}\} + [\bar{V}^f]\{\bar{f}\} + [\bar{V}^v]\{\bar{v}\} + [\bar{V}^w]\{\bar{w}\} - \lambda[\bar{Y}^v]\{\bar{v}\} = 0, \tag{29b}$$

$$[\bar{W}^e]\{\bar{e}\} + [\bar{W}^p]\{\bar{p}\} + [\bar{W}^f]\{\bar{f}\} + [\bar{W}^v]\{\bar{v}\} + [\bar{W}^w]\{\bar{w}\} - \lambda[\bar{Z}^w]\{\bar{w}\} = 0, \tag{29c}$$

$$[\bar{P}^p]\{\bar{p}\} + [\bar{P}^f]\{\bar{f}\} = [\bar{P}^v]\{\bar{v}\} + [\bar{P}^w]\{\bar{w}\}, \tag{29d}$$

$$[\bar{F}^p]\{\bar{p}\} + [\bar{F}^f]\{\bar{f}\} = [\bar{F}^v]\{\bar{v}\} + [\bar{F}^w]\{\bar{w}\}, \tag{29e}$$

where the vectors are defined as

$$\{\bar{e}\} = (e_c^1, e_s^1, e_c^2, e_s^2, \ldots, e_c^m, e_s^m)^{\mathrm{T}}, \text{ etc.}$$

and the coefficient matrices are all $(2m \times 2m)$ constant matrices, which are determined when deriving Eqs. (29a)–(29e).

Using Eqs. (29a), (29d) and (29e) to eliminate $\{\bar{e}\}$, $\{\bar{p}\}$ and $\{\bar{f}\}$ in Eqs. (29b) and (29c) gives an eigenvalue problem of a $(4m) \times (4m)$ matrix. For any given circumferential wave number n in Eqs. (23), the solution of the eigenvalue problem yields eigenvalues, the smallest of which, λ_n^*, is called the buckling load parameter corresponding to that n. The minimum of all these λ_n^* is the critical load parameter, λ_{cr}, of the shell, i.e.,

$$\lambda_{\mathrm{cr}} = \min_{n=1,2,\ldots} (\lambda_n^*). \tag{30}$$

Then, substitution of λ_{cr} into Eq. (25), where the values of P, Q and S are given for a specific problem, yields the critical loads.

5. Axisymmetric case

The case when $n = 0$ in Eq. (23) is referred to as axisymmetric case. In this case, all quantities are independent of y. The equations of buckled equilibrium become

$$\frac{\mathrm{d}T_x}{\mathrm{d}x} = 0, \tag{31a}$$

$$\frac{\mathrm{d}T_{xy}}{\mathrm{d}x} + \frac{Q_y}{R} + T_x^0 \frac{\partial^2 v}{\partial x^2} = 0, \tag{31b}$$

$$\frac{\mathrm{d}Q_x}{\mathrm{d}x} - \frac{T_y}{R} + T_x^0 \frac{\partial^2 w}{\partial x^2} = 0, \tag{31c}$$

$$\frac{\mathrm{d}M_x}{\mathrm{d}x} - Q_x = 0, \tag{31d}$$

$$\frac{\mathrm{d}M_{xy}}{\mathrm{d}x} - Q_y = 0. \tag{31e}$$

From these equations it can be seen that only the axial load contributes to the axisymmetric buckling. Eq. (31a) and the fact that $T_x(0) = T_x(L) = 0$, i.e., there is no change in the end load (since bifurcation is supposed to occur at a constant load), leads to the conclusion that $T_x(x) = 0$. Therefore,

$$\frac{\mathrm{d}u}{\mathrm{d}x} = -\frac{1}{A_{11}}\left(A_{12}\frac{w}{R} + A_{16}\frac{\mathrm{d}v}{\mathrm{d}x}\right). \tag{32}$$

Introducing Eqs. (9a), (9b) and (10) into Eqs. (31b)–(31e) and using Eq. (32) to eliminate u yield four governing equations:

$$\left(A_{66} - \frac{A_{16}^2}{A_{11}}\right)\frac{\mathrm{d}^2 v}{\mathrm{d}x^2} - \frac{A_{44}}{R^2}v + \frac{A_{11}A_{26} - A_{12}A_{16}}{RA_{11}}\frac{\mathrm{d}w}{\mathrm{d}x} + \frac{A_{44}}{R}\varphi - P\frac{\mathrm{d}^2 v}{\mathrm{d}x^2} = 0 \tag{33a}$$

$$\frac{A_{12}A_{16} - A_{11}A_{26}}{RA_{11}}\frac{\mathrm{d}v}{\mathrm{d}x} + A_{55}\frac{\mathrm{d}^2 w}{\mathrm{d}x^2} - \frac{A_{11}A_{22} - A_{12}^2}{R^2A_{11}}w - A_{55}\frac{\mathrm{d}\psi}{\mathrm{d}x} - P\frac{\mathrm{d}^2 w}{\mathrm{d}x^2} = 0 \tag{33b}$$

$$D_{11}\frac{\mathrm{d}^2\psi}{\mathrm{d}x^2} - A_{55}\psi + D_{16}\frac{\mathrm{d}^2\varphi}{\mathrm{d}x^2} - A_{55}\frac{\mathrm{d}w}{\mathrm{d}x} = 0 \tag{33c}$$

$$D_{66}\frac{\mathrm{d}^2\varphi}{\mathrm{d}x^2} - A_{44}\varphi + D_{16}\frac{\mathrm{d}^2\psi}{\mathrm{d}x^2} + A_{44}\frac{v}{R} = 0 \tag{33d}$$

in terms of four basic unknowns, $v(x)$, $w(x)$, $\Psi(x)$ and $\phi(x)$, where $P = -T_x^0$ is the axial compressive load. Eqs. (33a)–(33d) can be reduced to an eigenvalue problem of matrix by the five-point finite difference scheme described in the previous section.

6. Numerical examples

For the computation of numerical examples, two typical sets of boundary conditions are considered. One is called clamped and is expressed as

$$T_x = 0, \quad v = 0, \quad w = 0, \quad \psi = 0, \quad \varphi = 0 \quad \text{at } x = 0, L. \tag{34}$$

The other is called simply supported and is expressed as

$$T_x = 0, \quad v = 0, \quad w = 0, \quad M_x = 0, \quad \varphi = 0 \quad \text{at } x = 0, L. \tag{35}$$

Conditions in Eq. (34) are all in terms of the five basic unknowns and can be directly used in the solution procedure described in the previous sections. In conditions in (35), however, M_x is not one of the five unknown variables and the condition $M_x = 0$ should be transformed so as to be expressed by the basic unknowns:

$$D_{11}\frac{\mathrm{d}\psi}{\mathrm{d}x} + D_{12}\frac{\mathrm{d}\varphi}{\mathrm{d}y} + D_{16}\left(\frac{\mathrm{d}\psi}{\mathrm{d}y} + \frac{\mathrm{d}\varphi}{\mathrm{d}x}\right) = 0. \tag{36}$$

Substitution of Eq. (23) into Eq. (36) yields two equations

$$D_{11}p_c' + \frac{n}{R}(D_{12}f_s + D_{16}p_s) + D_{16}f_c' = 0 \quad \text{at } x = 0, L, \tag{37a}$$

$$D_{11}p_s' - \frac{n}{R}(D_{12}f_c + D_{16}p_c) + D_{16}f_s' = 0 \quad \text{at } x = 0, L \tag{37b}$$

for the finite difference scheme. Let $x = 0$ be station 0 and $x = L$ be station $m + 1$. Writing Eqs. (37a) and (37b) in forward finite difference at station 0 yields two algebraic equations, from which p_c^0 and p_s^0 can be solved. The solutions can be written in an enlarged matrix form, which reads, after taking into account $f_c^0 = f_s^0 = 0$ due to $\varphi = 0$ at $x = 0$

$$\begin{Bmatrix} p_c^0 \\ p_s^0 \\ \cdot \\ \cdot \\ \cdot \\ p_c^4 \\ p_s^4 \end{Bmatrix} = [L_p]\begin{Bmatrix} p_c^1 \\ p_s^1 \\ \cdot \\ \cdot \\ \cdot \\ p_c^4 \\ p_s^4 \end{Bmatrix} + [L_f]\begin{Bmatrix} f_c^1 \\ f_s^1 \\ \cdot \\ \cdot \\ \cdot \\ f_c^4 \\ f_s^4 \end{Bmatrix}, \tag{38}$$

where $[L_p]$ is a 10×8 matrix with its lower eight rows forming an eighth-order unit matrix, and $[L_f]$ is also a 10×8 matrix with its lower eight rows being all zero. A similar equation can also be established at station $m + 1$.

$$\begin{Bmatrix} p_c^{m-3} \\ p_s^{m-3} \\ \cdot \\ \cdot \\ \cdot \\ p_c^{m+1} \\ p_s^{m+1} \end{Bmatrix} = [R_p] \begin{Bmatrix} p_c^{m-3} \\ p_s^{m-3} \\ \cdot \\ \cdot \\ \cdot \\ p_c^{m} \\ p_s^{m} \end{Bmatrix} + [R_f] \begin{Bmatrix} f_c^{m-3} \\ f_s^{m-3} \\ \cdot \\ \cdot \\ \cdot \\ f_c^{m} \\ f_s^{m} \end{Bmatrix}, \tag{39}$$

where $[R_p]$ and $[R_f]$ are all 10×8 matrices with the upper part of $[R_p]$ being an eighth-order unit matrix and the upper part of $[R_f]$ being an eighth-order zero matrix. Eqs. (38) and (39) represent the condition $M_x = 0$ at $x = 0$ and L, and are used in the finite difference scheme.

The boundary conditions other than clamped and simply supported defined by Eqs. (34) and (35), if needed, can also be handled in a similar way.

Example 1. For a cylindrical shell, the plastic buckling under axial compression is mainly axisymmetric. In this example a set of three cylindrical shells tested by Lee (1962) resulting in axisymmetric buckling is used to check the present theory and the computer code. The stress–strain relation of the aluminium alloy used for the cylinders is expressed by the Ramberg–Osgood equation,

$$\varepsilon = \frac{\sigma}{E}\left[1 + \frac{3}{7}\left(\frac{\sigma}{\sigma_y}\right)^{N-1}\right], \tag{40}$$

where the three parameters are Young's modulus E, yield stress σ_y, and the hardening parameter N. Their values are $E = 70$ GPa, $\sigma_y = 23.62$ MPa and $N = 4.1$. The elastic Poisson's ratio is $v = 0.32$. The two ends of each shell are simply supported.

In Table 1, the experimental results of Lee (1962) and the calculated results with the present method are compared. Comparison shows that the deformation theory gives pretty good results but the flow theory predicts much too high critical loads. The three shells were also analyzed for axisymmetric buckling by Ore and Durban (1992). Their results are also listed in Table 1 and show good agreement with those from the present study.

Example 2. Another check of the present analysis is made with the experimental results of buckling due to pure torsion given by Lee and Ades (1957). The material used in their first group of tests is also described by the Ramberg–Osgood equation with $E = 70$ GPa, $\sigma_y = 503.66$ MPa and $N = 10$. The elastic Poisson's ratio is $v = 0.32$.

The cylinders used in the tests are fairly long with $L/R \approx 14$. Their thicknesses vary in a range. The two ends of each shell are simply supported. The calculated results are depicted in Fig. 1 together with the experimental ones. The figure shows a fairly good agreement between theoretical and experimental results, especially for the flow theory. It seems that for the plastic torsional buckling, the flow theory may predict critical loads better than the deformation theory.

Table 1
Critical stress (MPa) for pure axial compression

Geometry		Experimental (Lee 1962)	Present study		Ore and Durban (1992)	
R/h	L/R		Deform.	flow	Deform.	flow
9.36	4.21	96.87	89.71	165.46	88.49	162.33
19.38	4.10	78.60	74.87	124.25	74.09	122.03
29.16	4.06	64.74	67.70	106.00	67.06	103.98

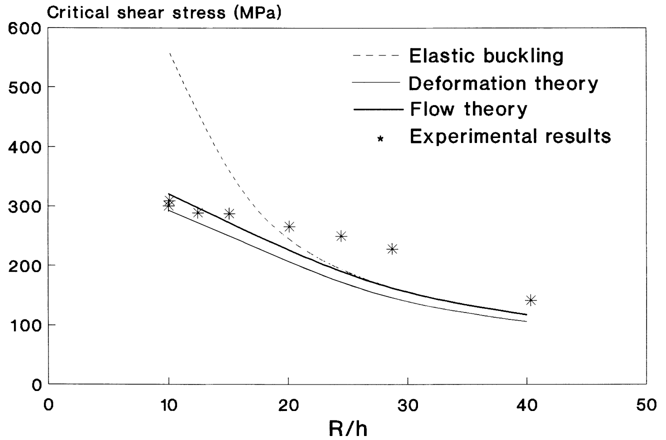

Fig. 1. Critical stress of torsional buckling of the shell in Example 2.

Example 3. In this example the buckling under combined axial and torsional loads is studied. The shells used in this example are the same as in Example 2, but with the ratio of radius to thickness fixed at $R/h = 15$.

As is known, for the buckling under combined loads, axial tension acts as a stabilizing factor while axial compression is a destabilizing factor. To show this, calculations were first made for the elastic buckling of the shells. The results are depicted by the solid curves in Figs. 2 and 3 showing that, compared with the buckling under pure torsion, the existence of axial compression reduces the critical shear stress and the existence of axial tension increases the critical shear stress. In this sense axial compression is said to be destabilizing and axial tension, stabilizing. Moreover, Fig. 2 shows that torsional load is also a destabilizing factor in terms of reducing the critical compressive stress compared with the critical stress of pure axial compression.

For plastic buckling, the interaction of axial and torsional loads are more complicated. First, the critical stresses for plastic buckling are lower than those for elastic buckling, and the above mentioned stabilizing and destabilizing effects are weaker for the lower stress level. Second, compared with each individual load,

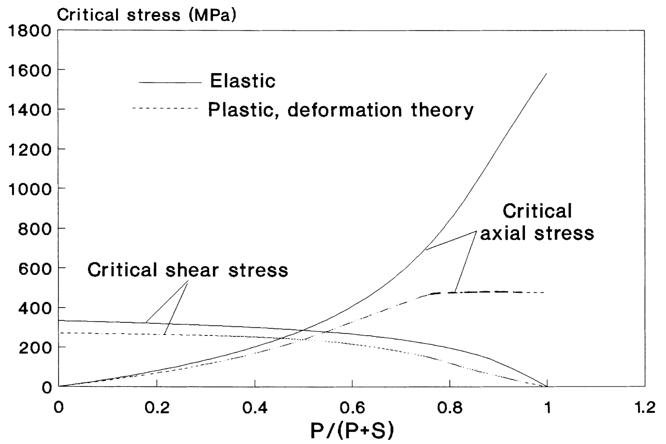

Fig. 2. Buckling under combined axial compression and torsion in Example 3. $P/(P+S)$ is a proportion parameter. $P/(P+S) = 0$ for pure torsion and $P/(P+S) = 1$ for pure axial compression. P and S are defined by Eq. (25).

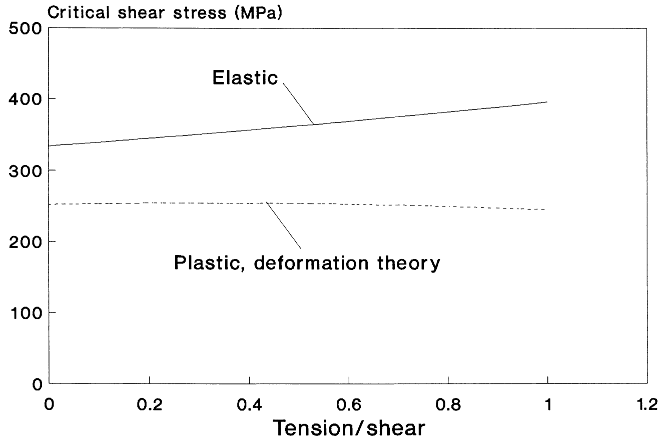

Fig. 3. Effect of the axial tension on the critical shear stress of the shell in Example 3.

combined loads tend to increase the plasticity and thus to reduce critical stresses. As a result of the combination of all these factors, the critical stresses for plastic buckling under combined axial and torsional loads are shown by broken curves in Figs. 2 and 3 and smooth curves in Figs. 4 and 5.

Tuğcu (1985) studied the interaction of axial and torsional loads for the plastic buckling of cylindrical shells by assuming a helical displacement field for buckling. Some of its results are listed in Tables 2 and 3, in comparison with the results based on the present study. These results are for the shell used by Tuğcu (1985) with the following geometrical and material parameters: $R/h = 20$, $L/R = 10$, $E/\sigma_y = 100, v = 0.3$, and $N = 6$, where N is the strain hardening parameter in Eq. (40). The two ends of the shell are assumed to be simply supported. The numerical results of Tuğcu (1985) listed in the tables are obtained from the curves in that paper.

For the deformation theory, as Table 2 shows, the results of the present study and those from Tuğcu (1985) are close to each other as long as the loading is identical or close to pure axial compression or pure torsion (when $T_x^0{:}T_{xy}^0 = 0{:}1, -0.1{:}1, 0.1{:}1, -1{:}0$ or $-1{:}0.1$, for example). For the loading in which T_x^0 and T_{xy}^0

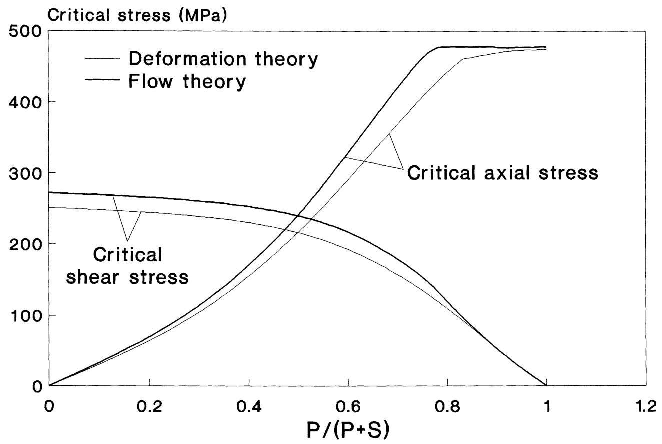

Fig. 4. Plastic buckling under combined axial compression and torsion in Example 3. $P/(P+S)$ is a proportion parameter. $P/(P+S) = 0$ for pure torsion and $P/(P+S) = 1$ for pure axial compression. P and S are defined by Eq. (25).

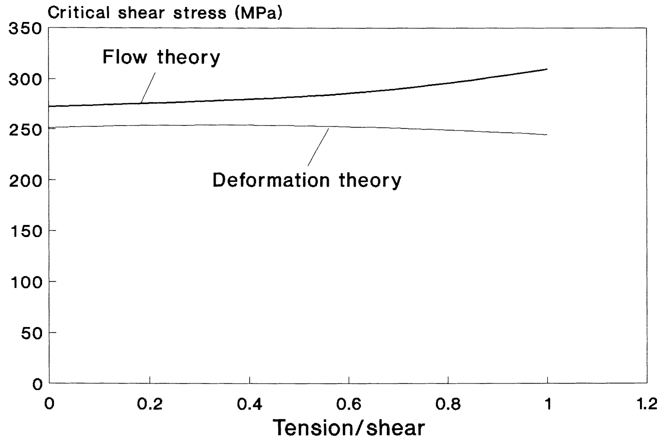

Fig. 5. Effect of the axial tension on the critical shear stresss at plastic buckling of the shell in Example 3.

Table 2
Comparison with Tuğcu (1985) for the deformation theory

T_x^0:T_{xy}^0	Present study		Tuğcu (1985)	
	σ_{cr}/σ_y	τ_{cr}/σ_y	σ_{cr}/σ_y	τ_{cr}/σ_y
−1:0	−1.62	0	−1.72	0
−1:0.1	−1.56	0.156	−1.66	0.166
−1:1	−0.742	0.742	−0.540	0.540
−0.1:1	−0.0839	0.839	−0.0836	0.836
0:1	0	0.840	0	0.834
0.1:1	0.0854	0.854	0.0826	0.826
1:1	0.807	0.807	0.551	0.551

Table 3
Comparison with Tuğcu (1985) for the flow theory

T_x^0:T_{xy}^0	Present study		Tuğcu (1985)	
	σ_{cr}/σ_y	τ_{cr}/σ_y	σ_{cr}/σ_y	τ_{cr}/σ_y
−1:0	−1.64	0	−2.364	0
−1:0.1	−2.14	0.214	−1.30	0.130
−1:1	−2.53	2.53	−0.492	0.492
−0.1:1	−0.110	1.10	−0.110	1.10
0:1	0	1.09	0	1.18
0.1:1	0.113	1.13	0.105	1.05
1:1	3.82	3.82	0.490	0.490

are comparable (T_x^0:$T_{xy}^0 = -1$:1 or 1:1, for example), Tuğcu (1985) predicts much lower critical stresses then the present study. Moreover, the results from Tuğcu (1985) do not show any stabilizing effect of axial tension while a bit of this effect can be seen from the results of the present study.

For the flow theory in Table 3, the results of the present study and those from Tuğcu (1985) are close to each other for the loading identical or close to pure torsion (T_x^0:$T_{xy}^0 = 0$:1, −0.1:1, or 0.1:1 for example). When the axial load is large (e.g. T_x^0:$T_{xy}^0 = -1$:0, −1:0.1, −1:1 or 1:1), Tuğcu (1985) predicts strong destabilizing effect no matter whether the axial load is compressive or tensile. The present study, however, while giving reasonable critical stress for pure compression, predicts strong stabilizing effect even in the case where the axial load is compressive. This strong stabilizing effect is quite different from the destabilizing effect shown in Fig. 4. This big difference confirms that the flow theory is very sensitive to the material properties and its practical performance is poor compared with the deformation theory.

Example 4. The shell used in this example is the same as the one in Example 1, but with $R/H = 20$ fixed. The results shown in Figs. 6–8 are based on the deformation theory.

Fig. 6 gives the critical stress of the shell subject to both axial and circumferential compressions. The parameter $P/(P+Q)$ used in Fig. 6 is similar to $P/(P+S)$ used in Fig. 4. It can be seen from Fig. 6 that the critical circumferential stress is not much affected by the existence of small axial compression, but on the other hand, the critical axial stress is quite sensitive to the existence of small circumferential compression. This can be explained by the dependence of the destabilizing mechanism on the stress level as mentioned in

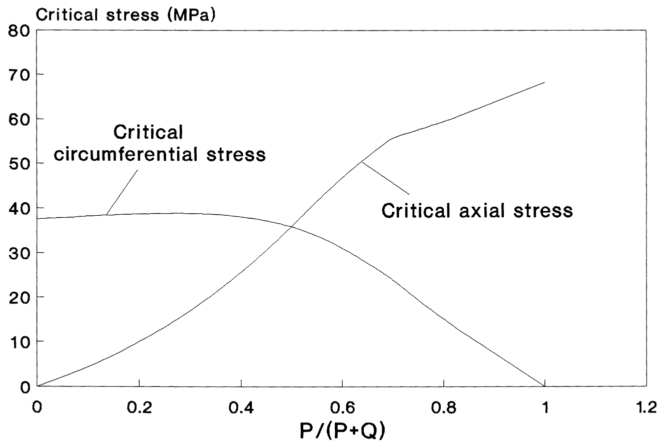

Fig. 6. Buckling due to biaxial compression in Example 4. $P/(P+Q)$ is a proportion parameter. $P/(P+Q) = 0$ for pure circumferential compression. $P/(P+Q) = 1$ for pure axial compression. P and Q are defined by Eq. (25).

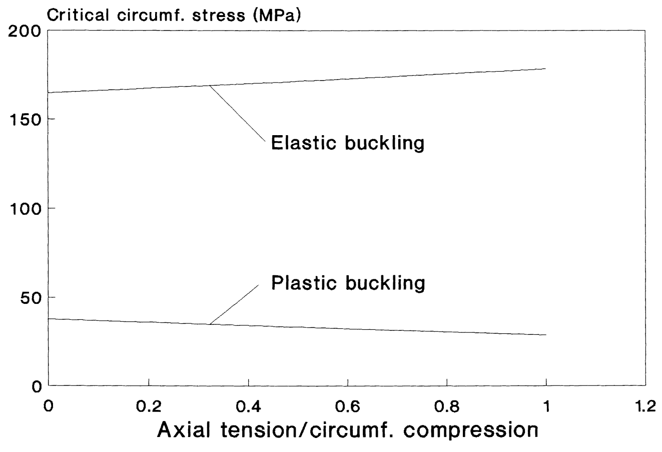

Fig. 7. Effect of axial tension on the critical stress of circumferential compression for the shell in Example 4.

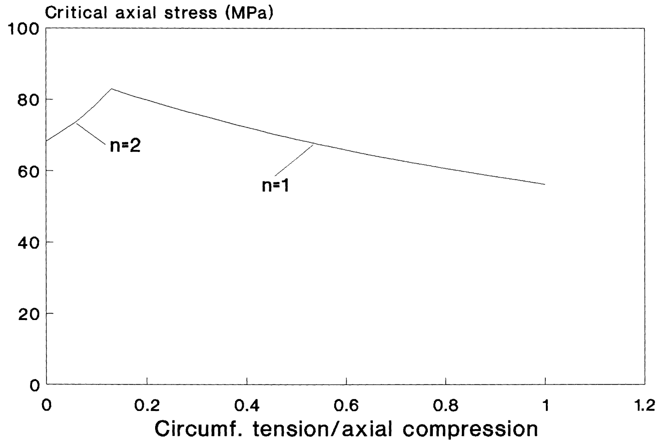

Fig. 8. Effect of circumferential tension on the critical stress of axial compression for the shell in Example 4.

the previous example. For an individual load of a combined loading system, the closer this load to its own elastic critical value, the stronger its destabilizing effect.

Fig. 7 depicts the influence of axial tension on the critical stress of circumferential compression. The curve for elastic buckling is for comparison. The comparison between the two curves in Fig. 7 shows that the stabilizing axial tension in elastic buckling becomes destabilizing in plastic buckling.

The curve in Fig. 8 is for the influence of circumferential tension on the critical stress of axial compression. It has two sections. The right section corresponds to wave number $n = 1$, which represents a column-type buckling of the shell. When the buckling mode transits from shell-type buckling with $n = 2$ to column-type buckling with $n = 1$, the stabilizing effect of circumferential tension disappears but the destabilizing effect due to increasing plasticity remains.

Acknowledgements

The authors wish to thank the Australian Research Council for the financial support for this project.

References

Andrews, K.R.F., England, G.L., Ghani, E., 1983. Classification of the axial collapse of cylindrical tubes under quasi-static loading. International Journal of Mechanical Science 25, 687–696.

Blachut, J., Galletly, G.D., James, S., 1996. Plastic buckling paradox for cylindrical shells. Proceedings of the Institution of Mechanical Engineers C210, 477–488.

Giezen, J.J., Babcock, C.D., Singer, J., 1991. Plastic buckling of cylindrical shells under biaxial loading. Experimental Mechanics 31, 337–343.

Hill, R., 1983. The Mathematical Theory of Plasticity. Oxford University Press, London (Chapter 2).

Lee, L.H.N., 1962. Inelastic buckling of initially imperfect cylindrical shells subject to axial compression. Journal of Aerospace Sciences 29, 87–95.

Lee, L.H.N., Ades, C.S., 1957. Plastic torsional buckling strength of cylinders including the effects of imperfections. Journal of Aerospace Sciences 24, 241–248.

Lin, M.C., Yeh, M.K., 1994. Buckling of elastoplastic circular cylindrical shells under axial compression. AIAA Journal 32, 2309–2315.

Mao, R., Williams, F.W., 1998a. Post-critical behaviour of orthotropic circular cylindrical shells under time dependent axial compression. Journal of Sound and Vibration 210, 307–327.

Mao, R., Williams, F.W., 1998b. Nonlinear analysis of cross-ply thick cylindrical shells under axial compression. International Journal of Solids and Structures 35, 2151–2171.

Ore, E., Durban, D., 1992. Elastoplastic buckling of axially compressed circular cylindrical shells. International Journal of Mechanical Science 34, 727–742.

Stein, M., 1986. Nonlinear theory for plates and shells including the effects of transvese shearing. AIAA Journal 24, 1537–1544.

Tabiei, A., Simitses, G.J., 1994. Buckling of moderately thick laminated cylindrical shells under torsion. AIAA Journal 32, 639–647.

Teng, J.G., Rotter, J.M., 1989. Non-symmetric bifurcation of geometrically nonlinear elastic–plastic axisymmetric shells under combined loads including torsion. Computers and Structures 32, 453–475.

Tuğcu, P., 1985. Bifurcation in elastic–plastic rotating shells under combined loading. Transactions of the CSME 9, 181–191.

Tuğcu, P., 1991. On plastic buckling predictions. International Journal of Mechanical Science 33, 529–539.